ARKIV FÖR FYSIK Band 12 nr 12

Communicated 13 February 1957 by MANNE SIEGBAHN and ERIK RUDBERG

Magnetic analysis of X-ray produced photo and Auger electrons

By EVELYN SOKOLOWSKI, CARL NORDLING and KAI SIEGBAHN

With 9 figures in the text

ABSTRACT

A precision method has been developed to determine atomic binding energies by means of magnetic analysis of photo electrons expelled from thin evaporated layers by X-radiation. The accuracy achieved in the present investigation is of the order of one electron volt, the limits being set essentially by the inherent widths of the atomic levels. The element copper has been studied and the K and L_{I} binding energies found are 8985.5 eV and 1100 eV respectively. Further, the KLL and KLM Auger spectra have been investigated. Seven well-resolved lines have been obtained in the KLL group. Earlier investigations have given only three KLL Auger lines in copper due to insufficient resolution, whereas theory indicates the possibility of ten lines in this group. Peaks due to electrons which have suffered discrete energy losses are observed on the low energy flanks of the photo lines.

A preliminary report of this investigation has been given in the *Physical Review* [1].

I. Introduction

Our present knowledge of the electronic structure of matter stems almost exclusively from X-ray studies. X-ray spectroscopy was developed to its inherent limits in the 1930's, and many of the problems which presented themselves at that time have not yet been solved. Thus, for instance, the "binding energies" obtained from X-ray absorption studies do not correspond to the absolute atomic binding energies. This is due to the fact that the absorbed radiation may excite the electrons of the shell under investigation into one of the upper levels or Fermi band. Further, these upper bands exhibit a pronounced structure and width, which reappears in the absorption edges, making it difficult to give an exact interpretation to the curves.

To circumvent these difficulties an alternative method of studying electronic structure was tried by de Broglie [2], Robinson *et al.* [3] and, later, by Ference [4]. Their method was based on the magnetic analysis of electrons expelled from a substance by X-radiation. However, the poor technique for particle detection, available at the time, together with deficiencies of the magnetic spectrometers used, prevented them from achieving an accuracy that could compete favourably with the older X-ray absorption methods.

In recent years, the development of precision nuclear spectroscopy has shown the above method in a new light. Nuclear spectrometers have already been employed for investigating e.g. the Auger effect in radioactive sources (see chapter XX in ref. [5]). The use of radioactive materials constitutes a rather serious limitation, however, since it is difficult to control the crystal structure and chemical composition of the sample without giving up the demands on high specific activity. Also, the internal conversion coefficients decrease rapidly with decreasing atomic number, causing intensity difficulties. Further, the halflife of the substance under investigation often makes it impossible to carry through the investigation on only one sample. Finally, a method using radioactivity is not applicable to investigations of absolute electron binding energies, since that would presuppose an exact knowledge of the nuclear energy levels, which in most cases we do not possess.

We have thought it worth while to develop further the method of magnetic analysis. Thus, an iron-free double-focussing β-spectrometer at this institute has been adapted for external conversion experiments, an X-ray tube, lowered into the spectrometer tank, constituting the "monochromatic" energy source.

If a quantum of energy $h\nu$ interacts with the electrons of a target material to give photo-effect,

$$h\nu = T_i + B_i,$$

where T_i is the kinetic energy of the electron emitted from the ith shell in a target atom and B_i is the total binding energy of an electron in that shell including the work function. By the method discussed in this paper, B_i can be determined uniquely to within an accuracy that is limited by the natural line width of the incident X-radiation and the atomic level to be examined. This energy, B_i, is a function not only of the element involved but also, to some extent, of the chemical composition and crystal structure of the sample. This is the case particularly for the outer electronic levels. Thus an accurate determination of B_i may give valuable information about the nature of chemical and crystal binding. Further, the results of such measurements may find application in the field of precision nuclear spectroscopy, where one determines the energies of conversion lines and, by adding the total electron binding energy, obtains the energy of the nuclear transition under investigation.

II. Apparatus

The spectrometer is that described by Siegbahn and Edvarson [6]. The magnetic field gives threedimensional focussing, which, at the relatively low intensities obtained in these experiments, is a great improvement over the instruments used by previous investigators [3, 4]. The sample holder has been replaced by the X-ray tube and converter described below. A GM-counter is used as a detector. Since, from the point of view of resolution, it is most favourable to work in as low an energy region as possible, care has been taken to reduce the cut-off of the counter window. For this purpose three to four layers of formvar film, with a total thickness of about 55 μg/cm^2 were used. A support for the window was made in the following way: A grid of nylon threads was held in place on a plane surface with tape and whetted with acetone, after which a celluloid frame was pressed on until the frame had dried. The support was then detached and the formvar films, floating on a water surface, could easily be transferred to it.

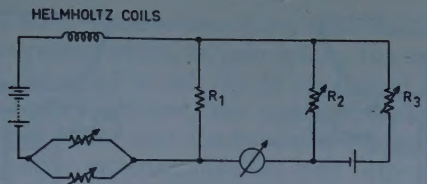

Fig. 1. Bridge circuit for control of current through the vertical Helmholtz coils.

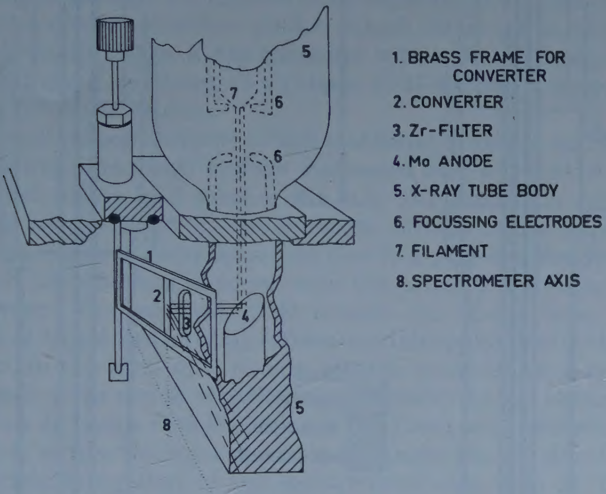

Fig. 2. The figure shows schematically the essential features of the X-ray tube and the converter mounting.

In the low energy regions investigated here the Helmholtz system [6], used to compensate undesirable magnetic fields, plays an essential role. Thus, at an energy of 7 keV a vertical field of 0.01 gauss would contribute 1 ‰ of the $B\varrho$ value. With the resolution used in the measurements no vertical external fields higher than 0.0002 gauss can be tolerated. To keep the compensating vertical Helmholtz field stable within this limit, even when the spectrometer field is superimposed, the bridge circuit shown in Fig. 1 is employed. In series with the vertical Helmholtz coils and regulating resistors there is a termostatically cooled 1 ohm precision resistor R_1. Prior to turning on the spectrometer the current through this circuit, ca. 2 amps, is adjusted with the aid of a millioerstedtmeter to give the correct compensation. The voltage drop over the 1 ohm resistor is then compensated by the voltage drop over the rheostat R_2. The rheostat circuit is fed by a 4 V battery and draws a current of about 1 mA. It has been found that at such a low load the battery voltage remains sufficiently constant during one measurement. Since the rheostats R_2 and R_3 are of the same type and magnitude and further are kept in the same container, temperature variations do not introduce an unbalance in the circuit. The only factor which may cause such an unbalance is a change in the Helmholtz current, which will then be registered as a deflection of the galvanometer. As already pointed out in ref. [6], the effect of the horizontal field components is less serious, so that these fields do not have to be kept

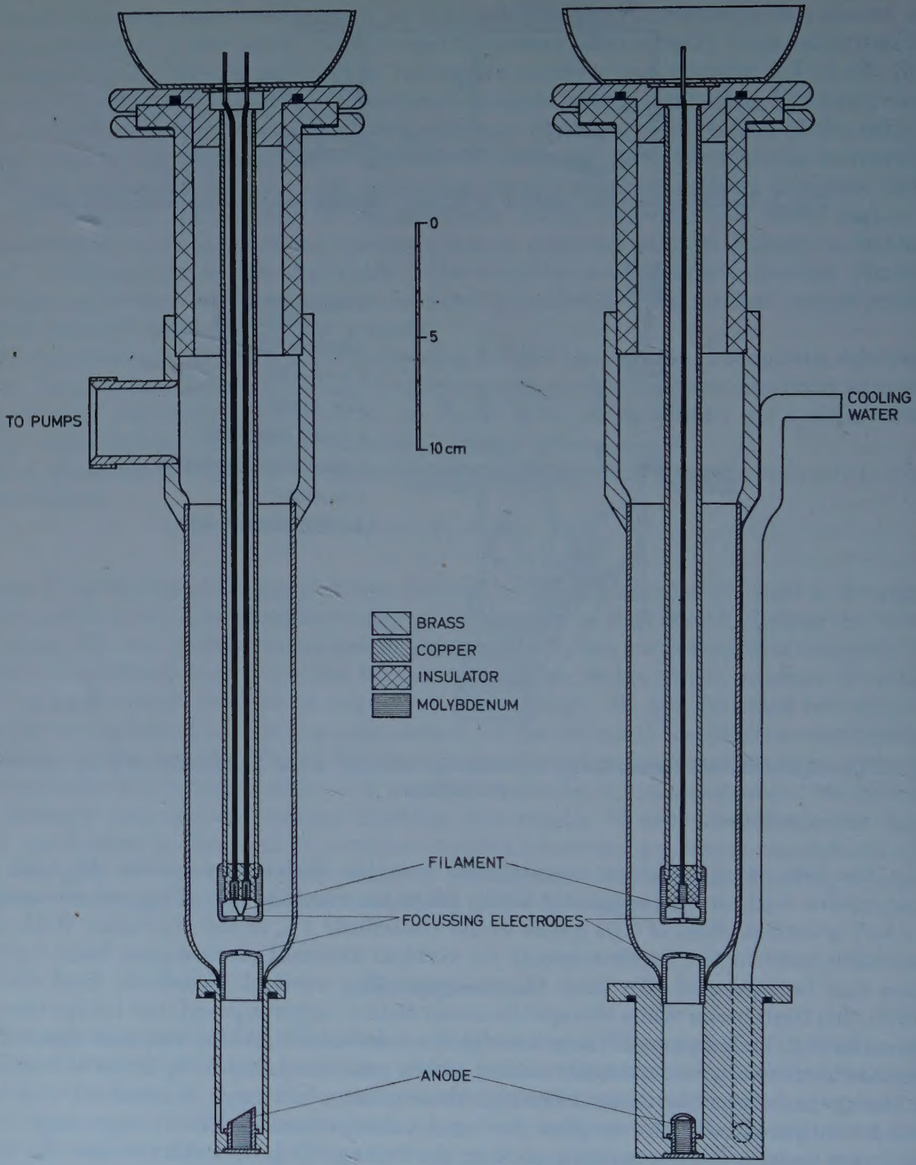

Fig. 3. X-ray tube.

under the same rigorous control. It should be mentioned that, besides the earth magnetic field, the stray field of a synchrocyclotron, situated some 75 meters away, gives a considerable contribution to the fields that have to be compensated.

The X-ray tube, made of copper to avoid magnetic materials, is shown in Figs. 2 and 3. Its construction was complicated by the fact that very little space was available in the spectrometer tank. The electron beam is focussed onto the anode electrostatically by means of a system, which, in principle, is the same as that of an axially symmetric electron gun described in ref. [7]. It consists of two approximately concentric spherical molybdenum surfaces, the upper of which is slightly adjustable along the tube axis. It was found that the focussing properties of the tube are very sensitive to the position of the emitting filament with respect to the upper electrode. For this reason a tungsten "hairpin" filament is employed, the emitting part of which is well defined and easy to keep in position. The whole assembly is easily accessible, and the anode can be changed for different experiments. The radiation is taken out of the tube through a critical absorber window which filters off the $K\beta$ components of the radiation. A study of the X-ray spectrum with a NaI (Tl) scintillation spectrometer showed that the X-ray tube, at a voltage of 45 kV and a current of 6 mA, was equivalent to a 600 curie source.

The negative high voltage supply[1] is well stabilized, giving a maximum voltage of 100 kV. The stability of the high voltage was tested over a period of 35 minutes at a value of 31 kV and with a load current of 3 mA. The maximum deviation from the mean during this time was 0.5 ‰. The emission current of the X-ray tube, having a maximum value of 25 mA, supplies a grid bias to a pentode, the output of which is fed back through transductors in series with the primary windings of the filament circuit transformer. The magnetic field outside the X-ray tube, induced by an emission current of 25 mA can have no influence on the properties of the spectrometer.

The converter, in the form of a narrow strip is mounted on a rectangular brass frame large enough so as not to contribute appreciably to the electron background. The frame makes a 45° angle with the plane of the X-ray tube exit window. Hence the outgoing radiation strikes the converter at a 45° angle, the 90° direction of optimum photo-electron yield being that of the spectrometer axis (Fig. 2). Converters were prepared by evaporating thin layers of the material under investigation onto 0.5 μ Al foils, 20 mm long and 0.7 mm wide. The evaporated layers were estimated to have a thickness of a few hundred Å.

III. Experimental results

The substance investigated in the present experiment was metallic Cu and the exciting X-radiation was that of Mo. Fig. 4 shows the main feature of the electron spectrum obtained under these conditions. Different groups of lines are distinguishable. These have their origin in two different effects: One is the photo-effect, where electrons in the shells of a Cu atom in its ground state are expelled by the incoming X-radiation, the other is the Auger-effect, where an already ionized atom makes a transition to a lower excited state by expelling an electron. It is clear that different information can be gained from these two effects about electronic binding. To the right in Fig. 4 are shown the two photo lines due to the conversion of the Mo $K\alpha_1$ and Mo $K\alpha_2$ radiation in the K-shell of Cu; to the left are shown the KLL and KLM Auger groups.

---

[1] The voltage- and current-supply for the X-ray tube was designed by Ing. Arne Bergquist, Stockholm.

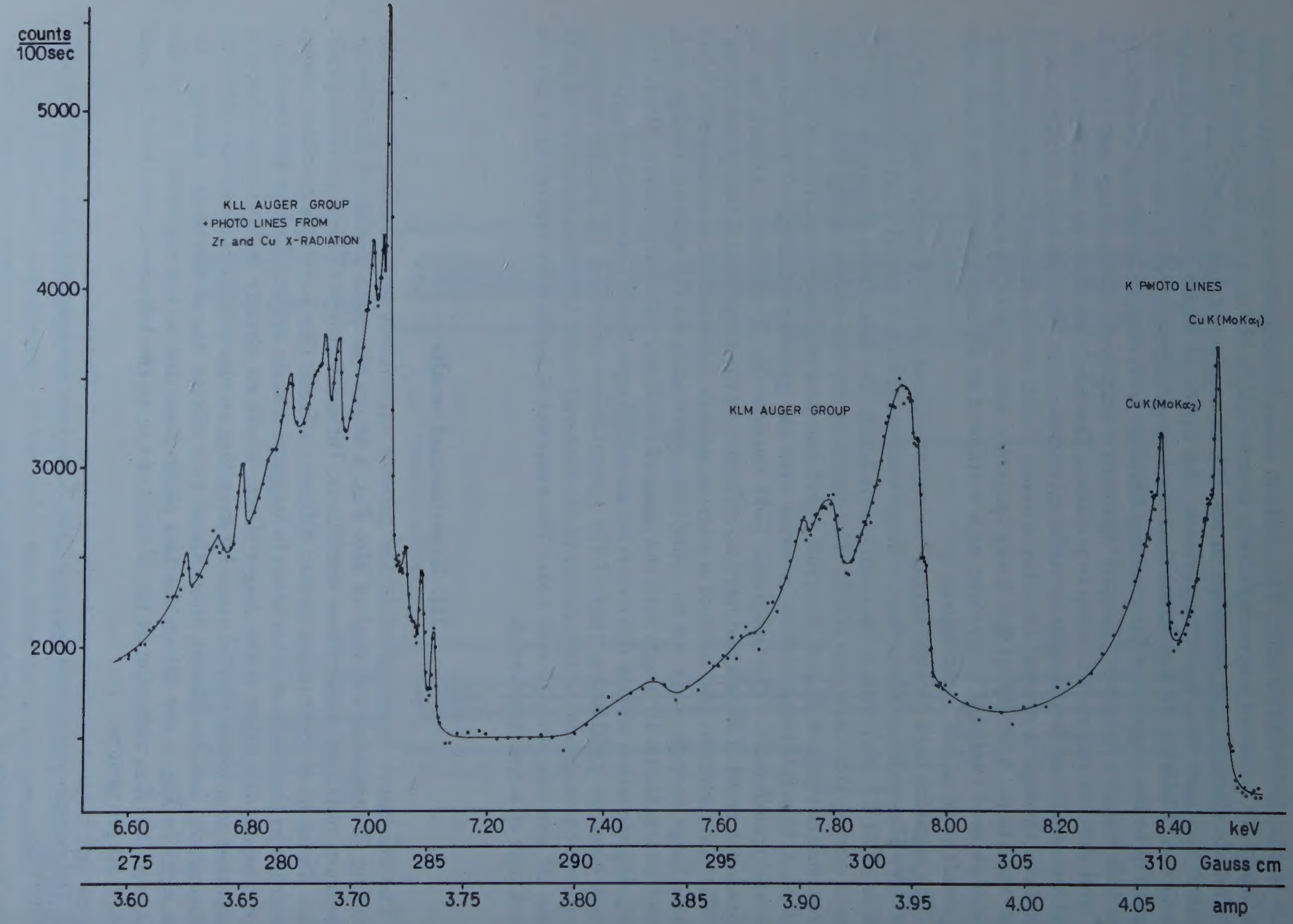

Fig. 4. Low energy region of the Cu spectrum, including the *KLL* and *KLM* Auger groups and the Cu *K* (Mo $K\alpha$) photo lines. The run

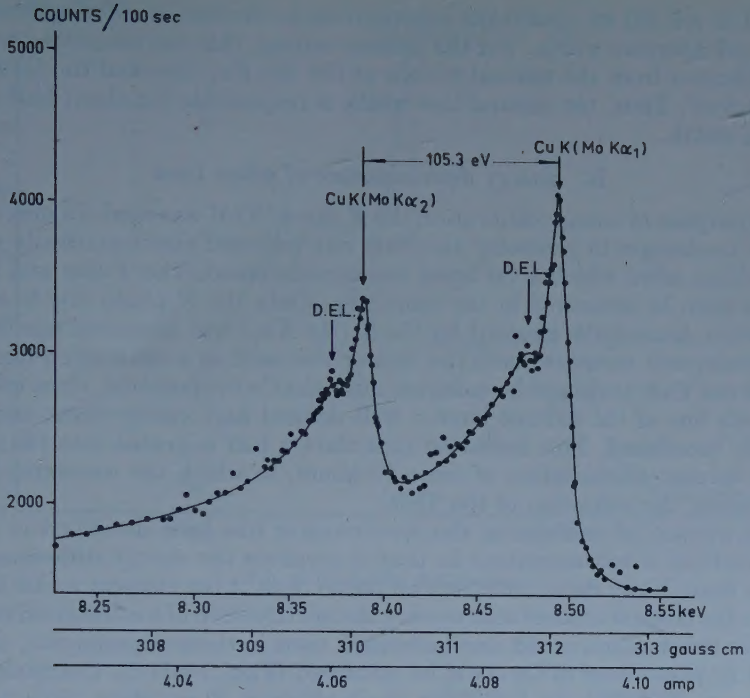

Fig. 5. Cu K (Mo $K\alpha_1$) and Cu K (Mo $K\alpha_2$) lines. The peaks denoted by D.E.L. are interpreted as due to discrete energy losses in the source in connection with inelastic scattering.

A. *Line width and resolution*

Fig. 5 gives the K photo " doublet" of Fig. 4 in greater detail and with better resolution. This figure is a good starting point for a discussion of the resolution and line widths in these experiments. On the low energy side of each line one can distinguish a satellite, which has been interpreted as due to K photo electrons, inelastically scattered in the source. It has been found in previous investigations [8] that such electrons suffer discrete energy losses of between 12 and 22 eV, depending on the scattering material. Various theories have been developed to explain these losses, some being based on collective electron interaction [9] and others on individual particle excitation [10]. There is a certain probability that an electron will suffer successive losses of this kind. This gives rise to a series of equidistant peaks, which decrease exponentially in height. The fact that only one hump (16 eV from the "undisturbed" electron peak) is observed in Fig. 5 can be explained by low intensity and greater width of the subsequent peaks and by the fact that the peaks due to the inelastically scattered electrons often exhibit an asymmetry on the low energy side. The probability of scattering and hence the contribution of these peaks to the total line intensity depends of course on the source thickness.

To find the contributions of the spectrometer setting and natural line widths to the over-all resolution one need only examine the high energy peak due to unscattered electrons. The experimental half-width of this peak is about 13 eV. From equation

34, Ch. III in ref. [5] we obtain the contribution to the line broadening from source, detector and aperture width. For the present setting, this was calculated to be 8 eV. The contribution from the natural widths of the Mo $K\alpha_1$, line and the Cu K level is also about 8 eV. Thus, the natural line width is responsible for about half of our experimental width.

B. *Energy determination of photo lines*

For the purpose of energy calibration the F-line of ThB was used. In order to avoid errors due to changes in geometry the ThB was collected electrostatically on a converter backing, after which a Cu layer was superimposed. The F-line and Cu photo lines could then be measured in the same run. (Only the K photo line from the Mo $K\alpha_1$ radiation, henceforth denoted by Cu K (Mo $K\alpha_1$) was measured against the F-line. In subsequent measurements the former was used as a calibration line.) It was noted that the ThB could not be collected after the Cu evaporation, since in that case the K photo line of Cu did not have a well defined high energy flank and became enormously broadened. This indicated that the Cu had migrated into the Al lattice under the intense α-irradiation of some 15 hours, to which the converter had been exposed during the collection of the ThB.

Another method of calibrating the spectrometer has been described in reference [6]. This method is self-consistent in that it employs the energy difference, known accurately from X-ray data, between two photo lines of the element under investigation. Thus, the method renders unnecessary the introduction of a calibration substance. In principle this method could also have been used in these experiments, since both the K and L_1 photo lines of Cu could be measured (Figs. 5 and 6). Unfortunately the $K-L_1$ energy difference for Cu is not available from X-ray data, since the corresponding transition is forbidden and other X-ray lines, which could be combined to give this energy, have not been measured with sufficient accuracy for low Z-values. A calculation shows that if the $K-L_{\mathrm{I}}$ energy difference were known with great accuracy the total errors pertaining to the "self-consistent" calibration method would in this case be somewhat less than those of the method used (see error discussion).

The line peaks have been taken to represent the positions of the lines. In the case of the K photo lines, the peaks are well defined within one twentieth of the half-width. The energy of the Cu K (Mo $K\alpha_1$) line is 8493.7 ± 1.0 eV ($B\varrho = 312.07$ gauss cm) and that of the Cu K (Mo $K\alpha_2$) line is 8388.4 ± 1.5 eV. If these energies are subtracted from the Mo $K\alpha_1$ and $K\alpha_2$ X-ray energies, two partly independent values of the Cu K binding energy are obtained. The latter are 8985.3 ± 1.0 eV and 8985.7 ± 1.5 eV. Taking the difference between the Cu K (Mo $K\alpha_1$) and the Cu K (Mo $K\alpha_2$) energies, the value 105.3 eV is obtained. This is in good agreement with the difference between the Mo $K\alpha_1$ and Mo $K\alpha_2$ lines as obtained from ordinary X-ray spectra, namely 104.9 eV.

The Cu L (Mo $K\alpha$) group is shown in Fig. 6. In this group the L_{I} "doublet" is the dominating, with an intensity about 4 times that of the unresolved L_{II}, L_{III} lines. From Fig. 6 a binding energy of 1100 ± 4 eV is obtained for the Cu L_{I} shell.

An unexpected check of the Cu K and L_{I} binding energies was provided by the presence of Zr and Cu X-radiation. The Zr radiation originated in the critical absorber which was probably struck by electrons scattered from the anode. The Cu radiation originated mainly in the copper holder that surrounded the anode (Fig. 3), and which was removed for the final measurement of the Auger spectrum (see below). The photo lines due to Zr- and Cu-radiation (see Fig. 8*a*) are listed in Table 1.

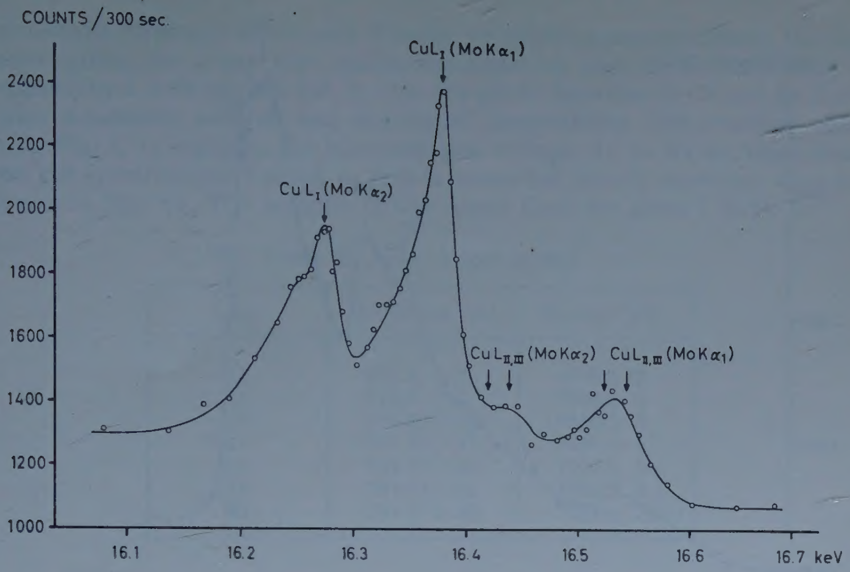

Fig. 6. Cu L (Mo $K\alpha$) group.

Table 1.

Line	$B\varrho$ (gauss cm)	Energy (eV)	Calculated energy (eV)
Cu L_{I}(Cu $K\alpha_1$)	282.01 ± .07	6947 ± 3	6947
Cu L_{I}(Cu $K\alpha_2$)	281.61 ± .08	6928 ± 4	6928
Cu L_{II}(Cu $K\alpha_1$)	284.97 ± .05	7092 ± 2.5	7090
Cu L_{III}(Cu $K\alpha_1$)	285.35 ± .05	7111 ± 2.5	7109
Cu K(Zr $K\alpha_1$)	278.76 ± .05	6789 ± 2.5	6787
Cu K(Zr $K\alpha_2$)	276.91 ± .05	6700 ± 2.5	6702

The values listed under "Calculated energy" are obtained from the data of the Cu (Mo $K\alpha$) lines given above, together with the energies of the Cu $K\alpha_1$, Cu $K\alpha_2$, Zr $K\alpha_1$ and Zr $K\alpha_2$ lines as obtained from X-ray studies [11]. It is to be noted that in this low energy region the Cu L_{II} and Cu L_{III} lines can be well resolved.

C. *Energy determination of Auger lines*

Theoretically, one is led to expect ten Auger lines in the *KLL* group (see below), and, with the resolution used in the present measurements, the hope that at least some of these should show up as well separated peaks is justified. The *KLM* Auger group is too complicated to be expected to yield much quantitative information. There are, however, indications of peaks in the *KLM* group at the energies listed in Table 2. Several of these peaks must be assumed to be composed of many unresolved lines (see Fig. 7).

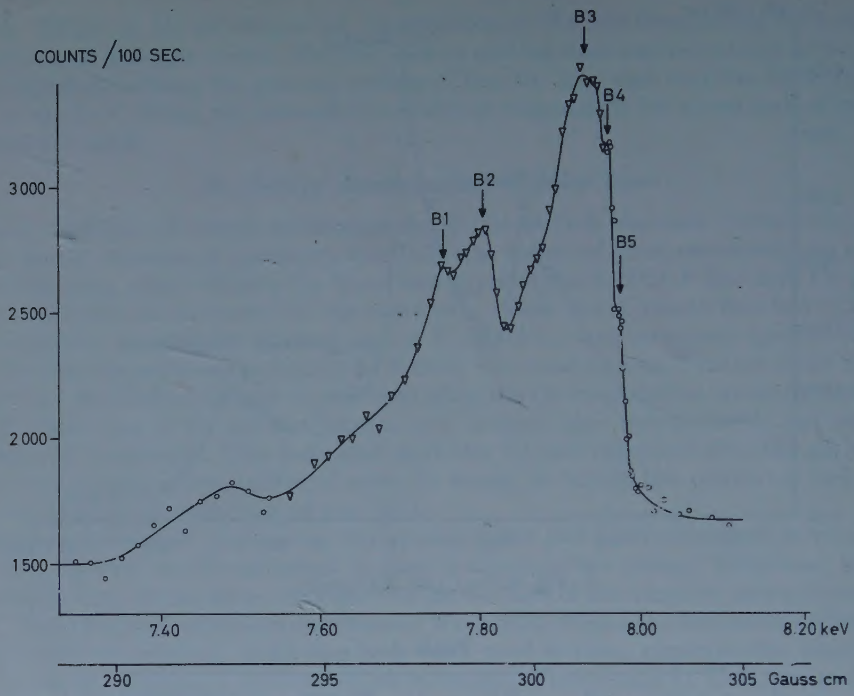

Fig. 7. *KLM* Auger group in Cu. (In the region plotted with triangles the statistics are twice as good as indicated by the ordinate.)

Table 2. *KLM* Auger group.

Line	$B\varrho$ (gauss cm)	Energy (eV)
*B*1	297.90	7745
*B*2	298.82	7793
*B*3	301.26	7920
*B*4	301.81	7949
*B*5	302.09	7963

The result of the first measurement of the *KLL* Auger group is shown in Fig. 8*a*. Of the fourteen lines obtained in this region six could immediately be interpreted as due to external conversion of Cu and Zr radiation. (See preceding section.) It may be pointed out that the Cu L_{II} (Cu $K\alpha_2$) photo line should have higher energy than line *A*7 and already for this reason cannot be identified with the latter. The energy and intensity of a seventh line leave little doubt that it is due to discrete energy losses (D.E.L.) in connection with inelastic scattering in the source. Thus there remain seven lines, which may still be interpreted as Auger lines. Several runs were made under identical conditions, and the spectrum was found to be reproducible. To exclude the possibility that the lines might originate in the converter backing or sample holder, the measurement was repeated without the evaporated copper layer.

In that case no structure was found. Finally, to obtain purer conditions, the copper ring surrounding the X-ray tube anode was removed, and the Zr filter (0.01 mm) was replaced by a 0.03 mm Nb foil, so that the photo lines due to Cu and Zr X-radiation were drastically reduced and eliminated, respectively. The resulting curve is shown in Fig. 8. It confirms the interpretation of lines *A*1 to *A*7 as Auger lines. In this run the spectrometer was set to give a somewhat poorer resolution than in the run shown in Fig. 8*a*. The energies of the Auger lines are given i Table 3.

Table 3. KLL Auger group.

Line	$B\varrho$ (gauss cm)	Energy (eV)
*A*1	277.4 ±.2	6735±12
*A*2	279.7 ±.2	6836± 9
*A*3	280.36±.08	6886± 4
*A*4	281.22±.15	6908± 8
*A*5	283.20±.05	7005± 2.5
*A*6	283.76±.05	7033± 2.5
*A*7	284.37±.05	7063± 2.5

It might be pointed out that Auger lines were found by Robinson and Young [3] at the following energies:

KLL group	*KLM* group
6839 eV	7730 eV
6986 eV	7891 eV
7060 eV	

However, some of these lines are described as doubtful and the reported errors in the energy values are up to 1:250.

D. *Intensity measurements*

The GM counter window (formvar) had a cut-off of slightly less than 4 keV. According to reference [12] this corresponds to an area density of approximately 55 μg/cm^2. Assuming the data for an aluminium-coated[1] collodion film of the same area density to be applicable to the window used, we find from the above reference that the window absorption becomes completely negligible at about 16 keV. Over the linear region of the absorption curve (i.e. between 4 and 7.3 keV) the change in transmission per 100 eV is roughly 2.5 per cent. Above 7.3 keV the slope decreases rapidly.

Another contribution to the errors in intensity is due to gradual variations in the X-ray intensity. The slow decrease in intensity was attributed to the formation of deposits of tungsten from the filament and of carbon on the anode. Over a period of five hours the intensity variation could be as great as ten per cent. As an illustration of an intensity estimate pertaining to a measurement made over a short period of time and small energy interval, it may be mentioned that an analysis of the curve in

---

[1] There has been no indication of a hysteresis effect in the window similar to that reported in ref. [12] for uncoated formvar films with an electron current of 10^{-10} amp. over a $\frac{1}{4}''$ diameter circle.

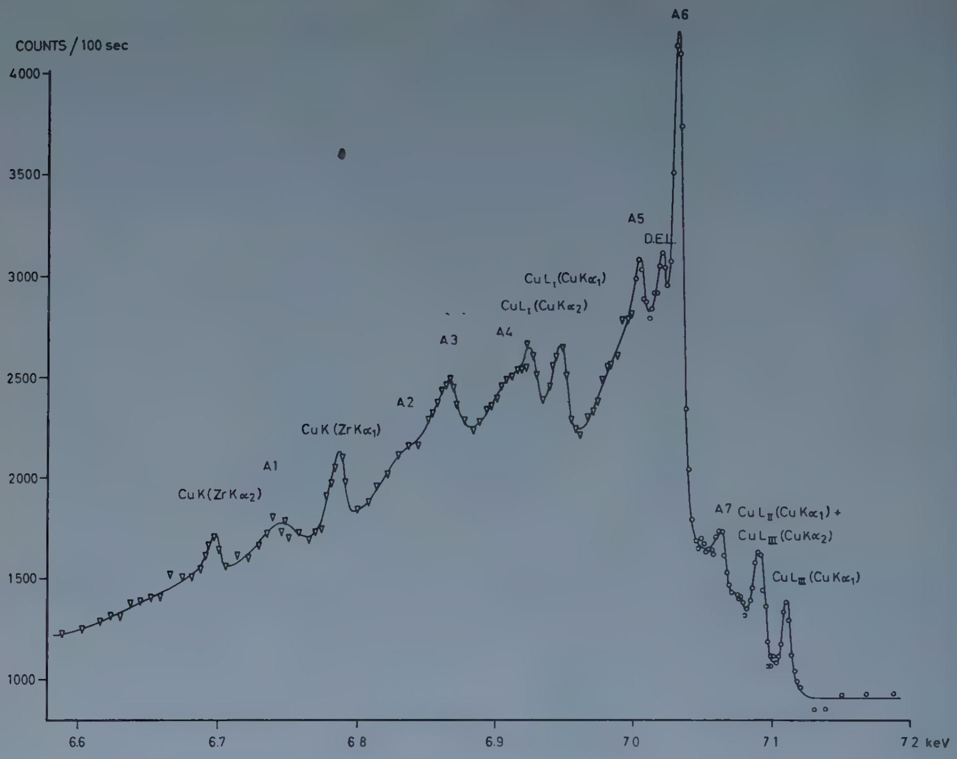
COUNTS / 100 sec
4000
3500
3000
2500
2000
1500
1000
6.6
6.7
6.8
6.9
7.0
7.1
7.2 keV
A6
A5
D.E.L.
CuL$_I$(CuKα_1)
CuL$_I$(CuKα_2)
A4
A3
A2
CuK(ZrKα_1)
A1
CuK(ZrKα_2)
A7
CuL$_{II}$(CuKα_1) +
CuL$_{III}$(CuKα_2)
CuL$_{III}$(CuKα_1)

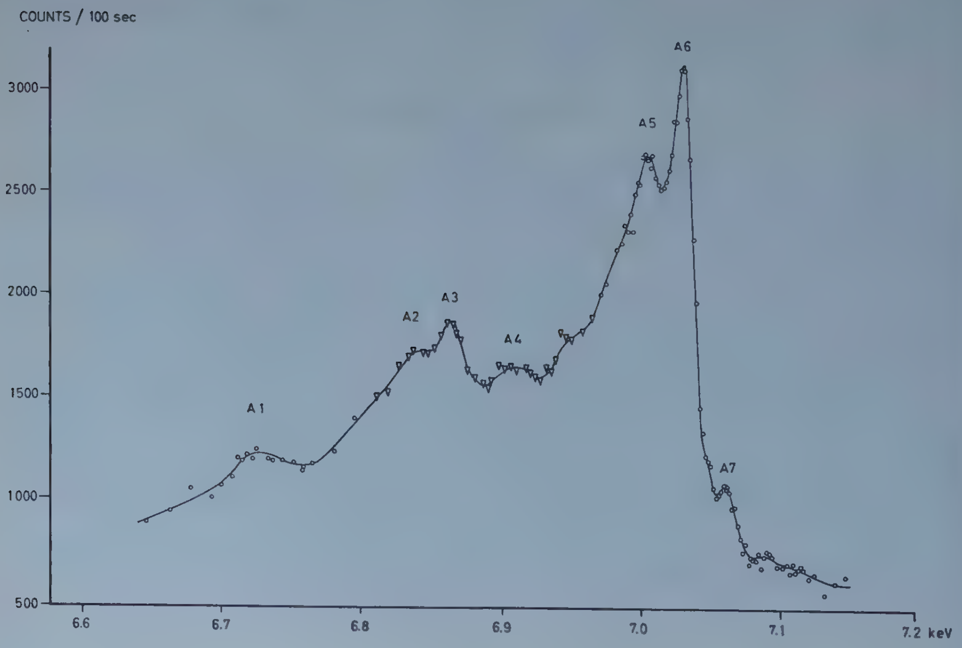
COUNTS / 100 sec
3000
2500
2000
1500
1000
500
6.6
6.7
6.8
6.9
7.0
7.1
7.2 keV
A6
A5
A3
A2
A4
A1
A7

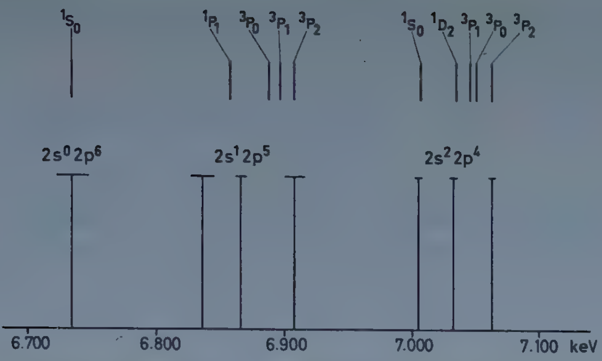
$^1S_0$
$^1P_1$ $^3P_0$ $^3P_1$ $^3P_2$
$^1S_0$ $^1D_2$ $^3P_1$ $^3P_0$ $^3P_2$
$2s^0 2p^6$
$2s^1 2p^5$
$2s^2 2p^4$
6.700
6.800
6.900
7.000
7.100 keV

Fig. 9. Schematic diagram showing the experimental Auger energies. Above the experimental groups are plotted the lines expected on theoretical grounds. The *relative* positions of the lines belonging to the same configuration have been calculated, whereas the *absolute* positions of the groups have been fitted to the experimental results in such a way that the lines of highest energy coincide. (See section IV.)

Fig. 5 gives for the ratio Cu (Mo $K\alpha_1$) to Cu (Mo $K\alpha_2$) the value 2.0 in good agreement with X-ray data for the $K\alpha_1$ and $K\alpha_2$ lines.

It is interesting to study the relative intensities of the different L photo lines. In the case where Mo $K\alpha_1$ radiation (of energy 17.479 keV) is converted, the L_{I} line is stronger than the unresolved $L_{\mathrm{II}}+L_{\mathrm{III}}$ group by about a factor 4, whereas in the case where Cu $K\alpha_1$ radiation (of energy 8.047 keV) is converted, the intensity ratios $L_{\mathrm{I}}:L_{\mathrm{II}}:L_{\mathrm{III}}$ seem to be closer to 1. A separate investigation of the relative L-line intensities as a function of the X-ray energy will be made.

It must be pointed out that it is not possible to measure *absolute* Auger yields simply by comparing the photo-line and Auger-line intensities, since the X-ray continuum contributes appreciably to the latter.

E. *Discussion of errors*

The procedure of determining the energy of a given line consists of two steps: (1) Finding the momentum ($B\varrho$) of the line by comparing its current value I to the current I_c of a calibration line, the momentum of which ($B\varrho_c$) is known. (2) Converting the momentum value $B\varrho$ into appropriate energy or frequency units. It is easily seen that the error pertaining to step 1 is

$$\frac{\Delta B\varrho}{B\varrho}=\frac{\Delta I}{I}+\frac{\Delta I_c}{I_c}+\frac{\Delta B\varrho_c}{B\varrho_c}. \tag{1}$$

In the errors of the experimental values given in the preceding sections we have only included the first two terms, since the errors in the $B\varrho$ value of the ThB F-line

---

Fig. 8. *KLL* Auger spectrum of Cu. In the upper curve (a) an admixture of photo lines was obtained because of the presence of Cu- and Zr X-radiation. The bottom curve (b) was taken up under purer conditions to facilitate the identification of the Auger lines. In the former run the spectrometer was set to give a somewhat better resolution. (In the regions plotted with triangles the statistics are twice as good as indicated by the ordinate.)

do not, in principle, place any limits on the method. $\Delta B\varrho_c/B\varrho_c$ is calculated in reference [6] and is shown to have the form

$$\frac{\Delta B\varrho_c}{B\varrho_c} = +3.3\frac{\Delta\alpha}{\alpha} + 0.65\frac{\Delta\bar{\nu}}{\bar{\nu}} + 0.65\frac{\Delta h/e}{h/e} + 0.35\frac{\Delta m/e}{m/e}, \tag{2}$$

where $\Delta\alpha/\alpha$ is an error pertaining to the current measurements and $\Delta\bar{\nu}/\bar{\nu}$ is the uncertainty in the frequency that corresponds to the energy difference between the K and $L_{\rm I}$ shells of Bi. Throughout we shall neglect the uncertainty in the velocity of light. From reference [6] we get that $\Delta\alpha/\alpha = 1.2\times10^{-5}$ and $\Delta\bar{\nu}/\bar{\nu} = 9\times10^{-5}$.

Assuming an unrelativistic treatment to be justified, we have the following relation between the frequency ν (in sec.$^{-1}$) and the momentum $B\varrho$:

$$\nu = \frac{1}{2}\,\frac{e}{m}\cdot\frac{e}{h}\,(B\varrho)^2. \tag{3}$$

Thus, the error pertaining to step 2 is

$$\frac{\Delta\nu}{\nu} = -\frac{\Delta m/e}{m/e} - \frac{\Delta h/e}{h/e} + 2\,\frac{\Delta B\varrho}{B\varrho}. \tag{4}$$

Combining expressions (1), (2) and (4) to give the *maximum* probable error we obtain

$$\frac{\Delta\nu}{\nu} = 6.6\,\frac{\Delta\alpha}{\alpha} + 1.30\,\frac{\Delta\bar{\nu}}{\bar{\nu}} + 0.30\,\frac{\Delta h/e}{h/e} + 0.30\,\frac{\Delta m/e}{m/e} + 2\,\frac{\Delta I}{I} + 2\,\frac{\Delta I_c}{I_c}. \tag{5}$$

For the uncertainties in the elementary constants we use the values given by DuMond and Cohen [13]:

$$\frac{\Delta h/e}{h/e} = 3.6\times10^{-5};\quad \frac{\Delta m/e}{m/e} = 2.8\times10^{-5}.$$

Further, $$\frac{\Delta I}{I} = 1:40\,000 \quad\text{and}\quad \frac{\Delta I_c}{I_c} = 1:33\,000.$$

Then $$\frac{\Delta\nu}{\nu} = 3.2\times10^{-4}$$

or 2.6 eV for the Cu K (Mo $K\alpha_1$) line.

If we take into account only those errors which are directly related to our measurements, i.e. if we neglect the errors in the $B\varrho$ value of the ThB F-line and the uncertainties in the elementary constants, we get (see equation (4))

$$\frac{\Delta\nu}{\nu} = 2\left(\frac{\Delta I}{I} + \frac{\Delta I_c}{I_c}\right) = 1.1\times10^{-4}$$

or 0.9 eV for the Cu K (Mo $K\alpha_1$) line.

Finally, if we wish to express the line energies in electron volts, we get for the total maximum probable error

$$\frac{\Delta E}{E} = \frac{\Delta h/e}{h/e} + \frac{\Delta \nu}{\nu} = 3.6 \times 10^{-4}$$

or 2.9 eV for the Cu K (Mo $K\alpha_1$) line.

Errors in the "self-consistent" calibration method (*see sec. III B*)

The coefficients in expression (2) for $B\varrho_c / B\varrho_c$ are those pertaining to the 239 keV line of ThB. In our case the expression for $\Delta B\varrho / B\varrho$ will be given by

$$\frac{\Delta B\varrho}{B\varrho} = 2.1 \frac{\Delta \alpha}{\alpha} + 0.52 \frac{\Delta \bar{\nu}}{\bar{\nu}} + 0.52 \frac{\Delta h/e}{h/e} + 0.47 \frac{\Delta m/e}{m/e}; \tag{6}$$

where

$$\frac{\Delta \alpha}{\alpha} = \frac{\Delta I_K}{I_K} + \frac{\Delta I_{L_I}}{I_{L_I}}.$$

This, combined with equation (4), gives

$$\frac{\Delta \nu}{\nu} = 4.2 \frac{\Delta \alpha}{\alpha} + 1.04 \frac{\Delta \bar{\nu}}{\bar{\nu}} + 0.04 \frac{\Delta h/e}{h/e} + 0.06 \frac{\Delta m/e}{m/e}. \tag{7}$$

If we assume that the uncertainty in $\bar{\nu}$ (i.e. the frequency corresponding to the energy difference between the K and L_I levels of Cu is negligible, then

$$\frac{\Delta \nu}{\nu} = 2.1 \times 10^{-4}$$

or 1.7 eV for the Cu K (Mo $K\alpha_1$) line.

It should be noted that all total errors given above are *linear* combinations of the partial errors and hence represent very generous estimates.

IV. Comparison of *KLL* data with theoretical results

An elementary discussion of the configurations involved in *KLL* Auger transitions has already been given in ref. [4]. In many, more recent, treatments (Ch. XX, ref. [5]) an entirely different approach has been made to the problem, which leads to a different result regarding the number and energy of the transitions. This latter approach does not seem entirely satisfactory, since it completely disregards the electron-electron interaction, and it may be justified to give a renewed discussion along the lines of ref. [4].

A *KLL* Auger transition in Cu takes place between the configurations

$$1s^1\ 2s^2\ 2p^6\ 3s^2\ 3p^6\ 3d^{10}\ 4s^1$$

and

$$1s^2 \left\{ \begin{matrix} 2s^0\ 2p^6 \\ 2s^1\ 2p^5 \\ 2s^2\ 2p^4 \end{matrix} \right\} 3s^2\ 3p^6\ 3d^{10}\ 4s^1.$$

Since a *KLL* transition does not change the *configurations* of the outer shells, we shall not consider these in the following discussion. For *extreme*[1] *j-j* coupling we get six alternatives for the final configuration:

$$1s^2 \left\{ \begin{array}{l} 2s^0_{1/2}\,2p^2_{1/2}\,2p^4_{3/2} \\ 2s^1_{1/2}\,2p^1_{1/2}\,2p^4_{3/2} \\ 2s^1_{1/2}\,2p^2_{1/2}\,2p^3_{3/2} \\ 2s^2_{1/2}\,2p^0_{1/2}\,2p^4_{3/2} \\ 2s^2_{1/2}\,2p^1_{1/2}\,2p^3_{3/2} \\ 2s^2_{1/2}\,2p^2_{1/2}\,2p^2_{3/2} \end{array} \right\} \ldots,$$

each of which corresponds to one energy state. The transitions from the initial state to these six possible final states have in previous treatments been denoted by

$$KL_{\mathrm{I}}L_{\mathrm{I}},\ KL_{\mathrm{I}}L_{\mathrm{II}},\ KL_{\mathrm{I}}L_{\mathrm{III}},\ KL_{\mathrm{II}}L_{\mathrm{II}},\ KL_{\mathrm{II}}L_{\mathrm{III}},\ \text{and}\ KL_{\mathrm{III}}L_{\mathrm{III}}$$

respectively.

However, it is known that extreme *j-j* coupling is practically an ideal case and that electron–electron interactions are far from negligible. The element copper represents an intermediate coupling between *j-j* and Russell–Saunders coupling. In the subsequent treatment we shall employ the Russell–Saunders notation of states but bear in mind that in reality the coupling is an intermediate one. Let us again consider the three possible final *L*-shell configurations. The resulting total *L*, *S* and *J* values and the different states corresponding to these configurations are given in Table 3.

Table 3.

Configuration	$2s^0\ 2p^6$	$2s^1\ 2p^5$				$2s^2\ 2p^4$				
L	0	1				0	2	1		
S	0	0	1			0	0	1		
J	0	1	2	1	0	0	2	2	1	0
State	$^1S_0$	$^1P_1$	$^3P_2$	$^3P_1$	$^3P_0$	$^1S_0$	$^1D_2$	$^3P_2$	$^3P_1$	$^3P_0$

It has been shown by several authors [14] that it is possible to calculate the separations of the terms of a given configuration for any intermediate type of coupling, if the exchange integrals for the wave functions pertaining to the vacancies in the closed shells and the spin-orbit interaction energies are known. Such calculations have been performed for the doubly ionized *L*-shell of copper by E. H. Kennard and E. Ramberg [15], who used the wave functions of Hartree [16]. The following expressions were given for the term separations in terms of the spin-orbit parameter A (throughout equal to $\frac{1}{3}$ of the $K\alpha_1$ and $K\alpha_2$ separation) and an exchange- and screening-parameter X.

---

[1] We take "extreme *j-j* coupling" to mean that the residual electrostatic coupling (i.e. over and above the averaged central field effects) between the different electrons is negligible compared with the spin-orbit coupling for each individual electron.

Configuration $2s^1\,2p^5$:

$$X = 41.5 \text{ eV}$$

$$^3P_2\text{–}^3P_1 : \Delta = \tfrac{1}{2}(X + 3A) - \tfrac{1}{2}[(X - A)^2 + 8A^2]^{\frac{1}{2}} = 11.0 \text{ eV}$$

$$^3P_2\text{–}^3P_0 : \Delta = 3A = 20.0 \text{ eV}$$

$$^3P_2\text{–}^1P_1 : \Delta = \tfrac{1}{2}(X + 3A) + \tfrac{1}{2}[(X - A)^2 + 8A^2]^{\frac{1}{2}} = 50.5 \text{ eV}$$

Configuration $2s^2\,2p^4$:

$$X = 6.89 \text{ eV}$$

$$^3P_1\text{–}^3P_2 : \Delta = (X - \tfrac{3}{2}A) - [(X - \tfrac{3}{2}A)^2 + 4XA]^{\frac{1}{2}} = -17.1 \text{ eV}$$

$$^3P_1\text{–}^3P_0 : \Delta = \tfrac{5}{2}X - [\tfrac{25}{4}X^2 - 5XA + 9A^2]^{\frac{1}{2}} = -4.5 \text{ eV}$$

$$^3P_1\text{–}^1D_2 : \Delta = (X - \tfrac{3}{2}A) + [(X - \tfrac{3}{2}A)^2 + 4XA]^{\frac{1}{2}} = 10.7 \text{ eV}$$

$$^3P_1\text{–}^1S_0 : \Delta = \tfrac{5}{2}X + [\tfrac{25}{4}X^2 - 5XA + 9A^2]^{\frac{1}{2}} = 38.7 \text{ eV}.$$

In principle it is possible to calculate the absolute energies of the states, but since the accuracy of the wave functions available is very poor, such calculations would be of little interest in connection with the experimental results. Fig. 9 shows schematically the spacing of the experimental Auger lines, together with the relative positions of the lines pertaining to the configurations $2s^1 2p^5$ and $2s^2 2p^4$ as calculated above. It is seen that the experimental lines fall into three distinct groups which must be interpreted as corresponding to the three possible configurations. The "group" having the lowest energy then corresponds to the $2s^0 2p^6$ configuration, which can only give rise to one state as shown in Table 3. The subsequent groups should give rise to four and five states respectively. Experimentally only three lines could be distinguished in each of these groups, which might be explained by insufficient resolution or by low intensity of some of the lines.

Institute of Physics, University of Uppsala.

REFERENCES

1. Nordling, C., Sokolowski, E., and Siegbahn, K., Phys. Rev. *105*, 1676 (1957).
2. de Broglie, M., and Thibaud, J. C. R., Acad. Sci. *180*, 179 (1925).
3. Robinson, H. R., Proc. Roy. Soc. *A 104*, 455 (1923).
   Robinson, H. R., and Cassie, A. M., Proc. Roy. Soc. *A 113*, 282 (1926).
   Robinson, H. R., and Young, C. L., Proc. Roy. Soc. *A 128*, 92 (1930).
4. Ference, M. Jr., Phys. Rev. *51*, 720 (1937).
5. Beta- and Gamma-Ray Spectroscopy, editor K. Siegbahn. North Holland Publishing Co, Amsterdam 1955.
6. Siegbahn, K., and Edvarson, K., Nuc. Phys. *1* 137 (1956).
7. Pierce, J. R., Theory and Design of Electron Beams. D. van Nostrand Co., 1949.
8. Haberstroh, G., Z. Physik *145*, 20 (1956).
9. Pines, D., Rev. Mod. Phys. *28*, 184 (1956).
10. Sternglass, E. J., Bul. Am. Phys. Soc., Series II, Vol. 1, 301 (1956).
11. Cauchois, Y., and Hulubei, C. R., Longeurs d'onde des émissions X et des discontinuités d'absorption X. Paris, Hermann, 1947.
12. Lane, R. O., and Zaffarano, D. J., Phys. Rev. *94*, 960 (1954).
13. DuMond, J., and Cohen R., Rev. Mod. Phys. *25*, 691 (1953).

14. HOUSTON, W. V., Phys. Rev. *33*, 297 (1929).
GOUDSMIT, S., Phys. Rev. *35*, 1325 (1930).
LAPORTE, O., and INGLIS, D. R., Phys. Rev. *35*, 1337 (1930).
15. KENNARD, E. H., and RAMBERG, E., Phys. Rev. *46*, 1040 (1934).
16. HARTREE, D. R., Proc. Roy. Soc. *A 141*, 282 (1933).
HARTREE, D. R., Proc. Roy. Soc. *A 143*, 506 (1934).

Tryckt den 27 maj 1957

Uppsala 1957. Almqvist & Wiksells Boktryckeri AB